SCIENTIFIC REPORTS

OPEN

SUBJECT AREAS:
ION TRANSPORT
ION CHANNELS IN THE NERVOUS SYSTEM
NEUROPHYSIOLOGY
MOLECULAR NEUROSCIENCE

Received
5 February 2013

Accepted
7 March 2013

Published
22 March 2013

Correspondence and requests for materials should be addressed to K.J.S. (swartzk@ninds.nih.gov)

Exploring structure-function relationships between TRP and Kv channels

Jeet Kalia & Kenton J. Swartz

Porter Neuroscience Research Center, Molecular Physiology and Biophysics Section, National Institute of Neurological Disorders and Stroke, National Institutes of Health 35 Convent Drive, Bethesda, Maryland 20892, USA.

The molecular mechanisms underlying the activation of Transient Receptor Potential (TRP) ion channels are poorly understood when compared to those of the voltage-activated potassium (Kv) channels. The architectural and pharmacological similarities between the members of these two families of channels suggest that their structure-function relationships may have common features. We explored this hypothesis by replacing previously identified domains and critical structural motifs of the membrane-spanning portions of Kv2.1 with corresponding regions of two TRP channels, TRPM8 and TRPV1. Our results show that the S3b-S4 paddle motif of Kv2.1, but not other domains, can be replaced by the analogous regions of both TRP channels without abolishing voltage-activation. In contrast, replacement of portions of TRP channels with those of Kv2.1 consistently yielded non-functional channels. Taken together, these results suggest that most structural elements within TRP channels and Kv channels are not sufficiently related to allow for the creation of hybrid channels.

Transient Receptor Potential (TRP) channels have been the intense focus of research since the first member was cloned in 1989[1]. Despite these efforts, the structural and mechanistic basis of TRP channel function remains poorly understood, in part because we currently have limited high resolution structural information on these channels[2]. In addition, TRP channels are modulated by a vast array of ligands possessing disparate physical and chemical characteristics, making it difficult to localize their binding sites and establish their mechanisms of activation. For example, TRPV1 is activated by stimuli as diverse as voltage, heat, protons, vanilloid compounds such as capsaicin and resiniferatoxin (RTX), and peptide toxins such as the double-knot toxin (DkTx) and vanillotoxins[3–6]. Another thermosensitive TRP channel, TRPM8, is activated by voltage, cold, and the small organic compounds, menthol and icilin[7]. How such a vast array of stimuli can activate these channels remains fascinating and poorly understood. Mutagenesis- and chimera-based approaches have identified regions of these channels that play critical roles in channel activation. For example, these approaches have been used to identify residues in TRPV1 that are critical for its activation by ligands such as capsaicin[8,9], RTX[9,10], DkTx[11], temperature[12–14] and pH[15]. Similar studies on TRPM8 have identified channel residues that are important for its activation by voltage[16] and its chemical agonists, icilin[17] and menthol[18]. Although this information is extremely valuable, it remains a challenge to discern whether the residues identified are directly involved in ligand binding or whether they influence an allosteric transition involved in channel gating. This task is especially non-trivial in the context of TRP channels because the gating elements in these channels remain largely unidentified.

In attempting to understand the principles underlying the activation of TRP channels, we sought to draw on our knowledge of voltage-activated potassium (Kv) channels, a family of ion channels that have been subject to extensive biophysical and structural investigation[19]. Several lines of evidence suggest that Kv channels and TRP channels may exhibit structural and functional similarities. First, members of both these channel families possess tetrameric architectures where each monomer consists of six transmembrane segments (S1–S6) with the S5–S6 region forming the pore (Fig. 1)[3,5,6,19,20]. Second, both TRP and Kv channels display pharmacological similarities, such as modulation by isostructural cystine knot peptide toxins—Kv channels are inhibited by voltage sensor-binding toxins[19,21], and TRPV1 is activated by double-knot toxin (DkTx)[11,22] and vanillotoxins[23]. Indeed, individual vanillotoxins have been reported to cross-react with TRPV1 and Kv2.1[23]. Another TRP channel, TRPA1, is activated by the tarantula toxin, GsMtx-4[24]. An additional pharmacological similarity between TRP and Kv channels is that members of both families are inhibited by internal quaternary ammonium ions[25–27]. A third line of evidence supporting similarities between TRP channels and Kv channels is that residues important for ligand-modulation of these channels map to similar regions. For example, residues in the S3–S4 region of TRPV1 (Fig. 2, green residues) play important roles in its activation by capsaicin and RTX[9,10], and several S3 and S4 residues of TRPM8 are important for menthol and icilin-sensitivity of the channel[16,18] (Fig. 2, orange and blue residues,

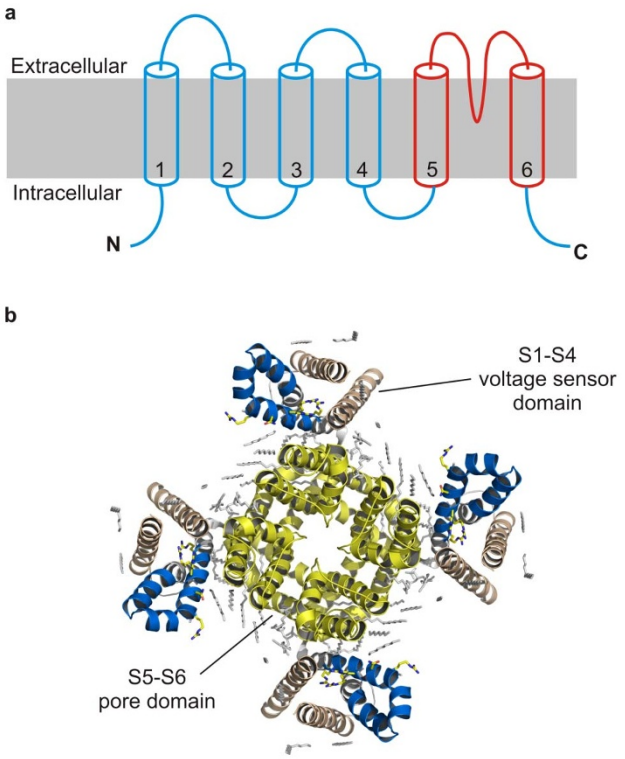

Figure 1 | Architecture of Kv and TRP channels. (a) Schematic representation of the transmembrane topology of channel subunits containing six transmembrane segments with the pore region formed by S5 and S6 segments shown in red. (b) Crystal structure of the tetrameric assembly of the Kv1.2–Kv2.1 chimera (Accession code 2R9R)[20] viewed from the extracellular side. The S3b–S4 paddle motif is shown in blue.

respectively). These regions overlap with the receptor for voltage sensor-targeting toxins in Kv channels—the S3b–S4 "paddle" (Fig. 1b; Fig. 2, gray highlighted region), a helix-turn-helix motif that moves in response to changes in membrane voltage to drive opening of the channel[19,28–35]. Fourth, charge-neutralizing mutations of positively charged residues in the S4 helix of TRPM8 have been shown to reduce the amount of charge that moves during voltage-activation of the channel[16], suggesting that this TRP channel's S4 helix may function as a voltage sensor, similar to what has been established in Kv channels[19,36–38]. Finally, studies on TRPV1[26,39] demonstrate that the internal pore is formed by S6 and that it opens and closes in response to capsaicin or voltage, paralleling the evidence for the S6 region of Kv channels forming the pore and serving as a gate that limits the flow of ions in the closed states[40]. Collectively, these intriguing observations support the idea that the transmembrane regions of TRP channels and Kv channels may have similar structures and that their mechanisms of gating may be related.

In the present study we explored the relationships between TRP channels and Kv channels using a chimera approach to determine whether structural motifs can be transferred between the two families of cation channels without disrupting function. Our efforts were motivated by previous chimera studies on a range of distantly related voltage-activated ion channels and voltage sensing proteins that have provided valuable information on structural relationships and in defining domains or motifs that serve specific functions[32,34,41,42].

Results

We decided to focus our efforts on the Kv2.1 channel and on two TRP channels, TRPV1 and TRPM8. We chose Kv2.1 because the gating properties of this Kv channel can be modulated by an array of peptide toxins that interact with the S1–S4 voltage-sensing domain[21], and because earlier studies have successfully used this channel to generate chimeras with other voltage-activated cation channels and voltage-sensitive proteins[32,34]. Our choice of TRPV1 was motivated by the availability of a large number of pharmacological tools targeting this channel, including vanilloid compounds and DkTx[4,6,11,22]. TRPM8 was an obvious choice for our studies because an earlier report suggested similar voltage-sensing mechanisms in this channel and Kv channels[16].

Fig. 2 shows the primary sequence alignment used to generate chimeras, covering the S1-S6 transmembrane segments of TRPV1, TRPM8 and Kv2.1, along with a variety of other tetrameric cation channels and voltage-sensitive proteins, including those for which X-ray structures are available[20,28,43–45]. Fig. 3 summarizes all 50 chimeras that we generated, and provides the specific boundaries for regions within the S1–S6 segments that were transferred between Kv2.1 and either TRPV1 or TRPM8. Unless otherwise stated, channel constructs were investigated by injecting cRNA into oocytes and performing two-electrode voltage clamp recordings to investigate their functional properties.

S3-S4 chimeras between TRPM8 and Kv2.1. The S3b–S4 paddle motif in Kv channels is extremely tolerant to protein engineering because it is relatively structurally unconstrained, making few contacts with other parts of the protein[20,28,29,32,34,43]. Indeed, in earlier work, the paddle region of Kv2.1 was replaced by the paddle regions of other voltage-gated channels such as the prokaryotic Kv channel, KvAP, Nav channels, the voltage-activated proton channel Hv1, and the voltage-sensitive phosphatase Ci-VSP, without destruction of voltage-activation and with concomitant transfer of pharmacology[32,34]. Due to its functional and pharmacological importance, and its tolerance to replacement, we first focused on making chimeras by replacing the paddle region of Kv2.1 with the corresponding regions of TRPV1 and TRPM8.

We generated twelve chimeras in which different portions of the Kv2.1 paddle were replaced with portions of the putative S3–S4 region of TRPM8 (Fig. 3d; 1–12M8Kv). Seven of these chimeras gave rise to functional channels (Fig. 3d; green dots) that were activated by membrane depolarization and that were sensitive to the selective Kv channel blocker, agitoxin2[46]. The voltage-activated currents observed for these chimeras exhibited a reversal potential of ~ -20 mV, consistent with the expected value for K^+−selective channels for the recording solution we used. All of these functional chimeras involved replacing regions within and immediately N-terminal to the paddle region (2M8Kv, 3M8Kv, 5M8Kv, 7M8Kv, 8M8Kv, 11M8Kv, and 12M8Kv), whereas those that failed to form functional channels (1M8Kv, 4M8Kv, 6M8Kv, 9M8Kv, and 10M8Kv) involved the transfer of regions extending beyond previously defined boundaries of the paddle motif[32].

Two of the largest functional paddle chimeras were 8M8Kv, a construct in which 31 residues of the paddle were replaced by 34 residues of TRPM8, and 3M8Kv, a construct in which 37 residues of Kv2.1 were replaced by 40 residues of TRPM8 (Fig. 4a). Although both of these chimeras were activated by membrane depolarization, their gating characteristics were different from those of Kv2.1. Indeed, both the chimeras exhibited much slower rates of activation and deactivation (Fig. 4b, c, and d; note differences in scale bars) and their conductance-voltage (G–V) relations had much shallower slopes compared to that of Kv2.1 (Fig. 4e). Fitting of a Boltzmann function to the G–V data for 3M8Kv and 8M8Kv yielded slopes (z) of 1.5 and 1.7, respectively, as compared to 3.2 for Kv2.1 (Fig. 4e; Table 1). One possible explanation for the reduced z values of these chimeras is that the three outer arginine residues in the S4 helix of Kv2.1 were replaced by only one positively charged residue in the transplanted region of TRPM8 (Fig. 4a). The energetics of gating were also perturbed in these chimeras; whereas 8M8Kv could be activated by a voltage stimulus lower than that required to activate

Figure 2 | Sequence alignment of six transmembrane-tetrameric ion channels and voltage-sensitive proteins. Residues of TRPV1 and TRPM8 that are identical or similar to those of Kv2.1 to which they are aligned are shown in bold lettering. The residues belonging to the selectivity filter region of each channel are underlined. Conserved residues that are important for voltage sensing in voltage-activated ion channels are depicted in red. TRPV1 residues shown in green are important for vanilloid sensitivity and those highlighted in yellow background are critical for DkTx sensitivity. TRPM8 residues shown in blue and orange are important for icilin and menthol sensitivity, respectively. A portion of the unusually long linker between the S5 and S6 helices of rNav1.2 (marked by an asterisk) is shown separately at the bottom for clarity.

Kv2.1, 3M8Kv required stronger depolarizations to elicit voltage-activated currents (Fig. 4e; Table 1). The large rightward shift of the G–V relationship of 3M8Kv precludes utilization of agitoxin2 to subtract background currents because the toxin unbinds at the higher voltages required to activate this chimera. Interestingly, this chimera remains constitutively open and cannot be closed entirely by membrane hyperpolarization, giving rise to a steady holding current (Fig. 4d and f) and non-zero conductance values at negative voltages (G–V plot in Fig. 4e). To verify that this holding current arises from the chimera, we applied agitoxin2 and observed that the holding current was reduced to negligible values (not shown).

In addition to playing important roles in sensing voltage, the S4 helix of TRPM8 is thought to be important for menthol sensitivity[16], raising the possibility that the transferred region of TRPM8 may confer ligand sensitivity to the chimeras. We therefore examined the sensitivity of the functional chimeras to menthol and in each case external application of the TRPM8 agonist was without effect. Voltage-activated currents before and after menthol treatment for our largest paddle chimera, 3M8Kv, are depicted in Fig. 4f.

If the S4 helix of TRPM8 serves as the voltage sensor of TRPM8, we might expect a TRPM8 variant containing a larger number of positively charged residues to display steeper voltage-dependent gating.

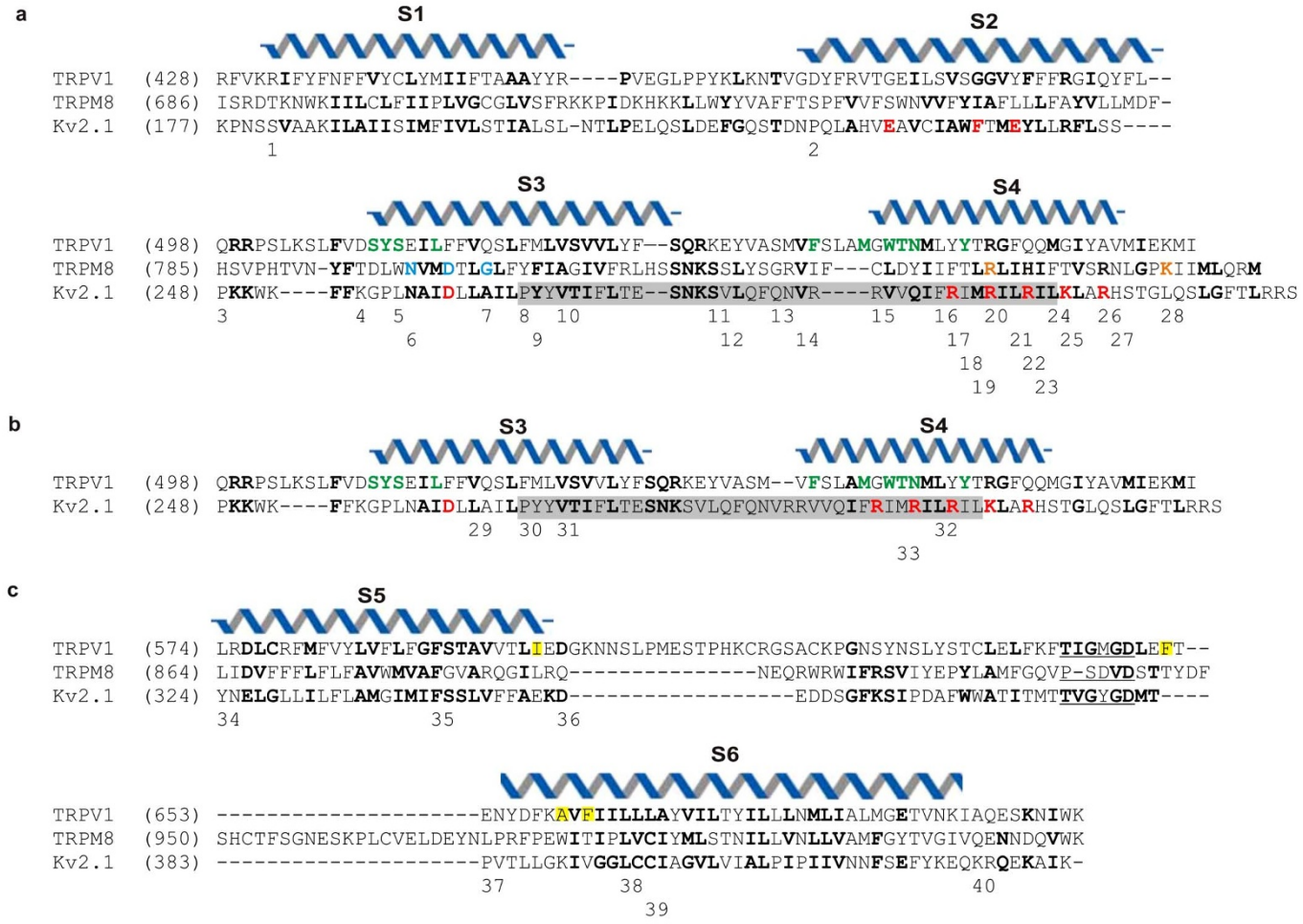

d

	TRPM8 in Kv 2.1	TRPV1 in Kv 2.1	Kv2.1 in TRPM8	Kv2.1 in TRPV1
S3-S4 chimeras	(6, 11) 1M8Kv (7, 11) 2M8Kv (7, 21) 3M8Kv (7, 22) 4M8Kv (9, 24) 5M8Kv (9, 25) 6M8Kv (10,19) 7M8Kv (10,21) 8M8Kv (10,26) 9M8Kv (20,28) 10M8Kv (13,21) 11M8Kv (14,22) 12M8Kv	(8, 21) 1V1Kv (10,21) 2V1Kv (29,32) 3V1Kv (30,33) 4V1Kv (30,32) 5V1Kv (31,32) 6V1Kv	(10,21) 1KvM8 (12,18) 2KvM8 (17,26) 3KvM8 (20,26) 4KvM8	(10,21) 1KvV1 (15,23) 2KvV1 (17,27) 3KvV1 (31,32) 4KvV1
S2-S3 chimeras	-	(3, 4) 7V1Kv (3, 5) 8V1Kv	-	-
S1-S4 chimeras	(1, 21) 13M8Kv (1, 27) 14M8Kv	(1,21) 9V1Kv (1,27) 10V1Kv	(1,21) 5KvM8 (1,27) 6KvM8	(1, 21) 5KvV1 (1, 27) 6KvV1
S2-S4 chimeras	(2, 21) 15M8Kv	(2,21) 11V1Kv	(2, 21) 7KvM8	(2, 21) 7KvV1
S5-S6 chimeras	(34, 40) 16M8Kv (35, 39) 17M8Kv (36, 37) 18M8Kv	(34,40) 12V1Kv (35,38) 13V1Kv (36,37) 14V1Kv	(34, 40) 8KvM8 (36, 37) 9KvM8	(34, 40) 8KvV1 (36, 37) 9KvV1

Figure 3 | Chimeras generated and characterized in this study. (a) Alignment of S1–S4 regions of TRPV1, TRPM8 and Kv2.1 used for generating most chimeras. (b) An alternate alignment of the S3–S4 regions of TRPV1 and Kv2.1. (c) Alignment of the S5–S6 regions for TRPV1, TRPM8 and Kv2.1. The numbers below specified residues in the alignment of the channels denote the start or end sites of the swapped regions. (d) Summary of chimeras generated in this study. Red dots indicate non-functional chimeras whereas green dots indicate functional chimeras. The chimeras are named using the code: (a, b) XC1C2, where numbers 'a' and 'b' correspond to the N-terminal residue and the C-terminal residue respectively of the transferred segment, 'X' is the serial number, 'C1' is the abbreviation for the donor protein and 'C2' is the abbreviation for the acceptor protein. Abbreviations for the proteins are: M8 for TRPM8, V1 for TRPV1 and Kv for Kv2.1.

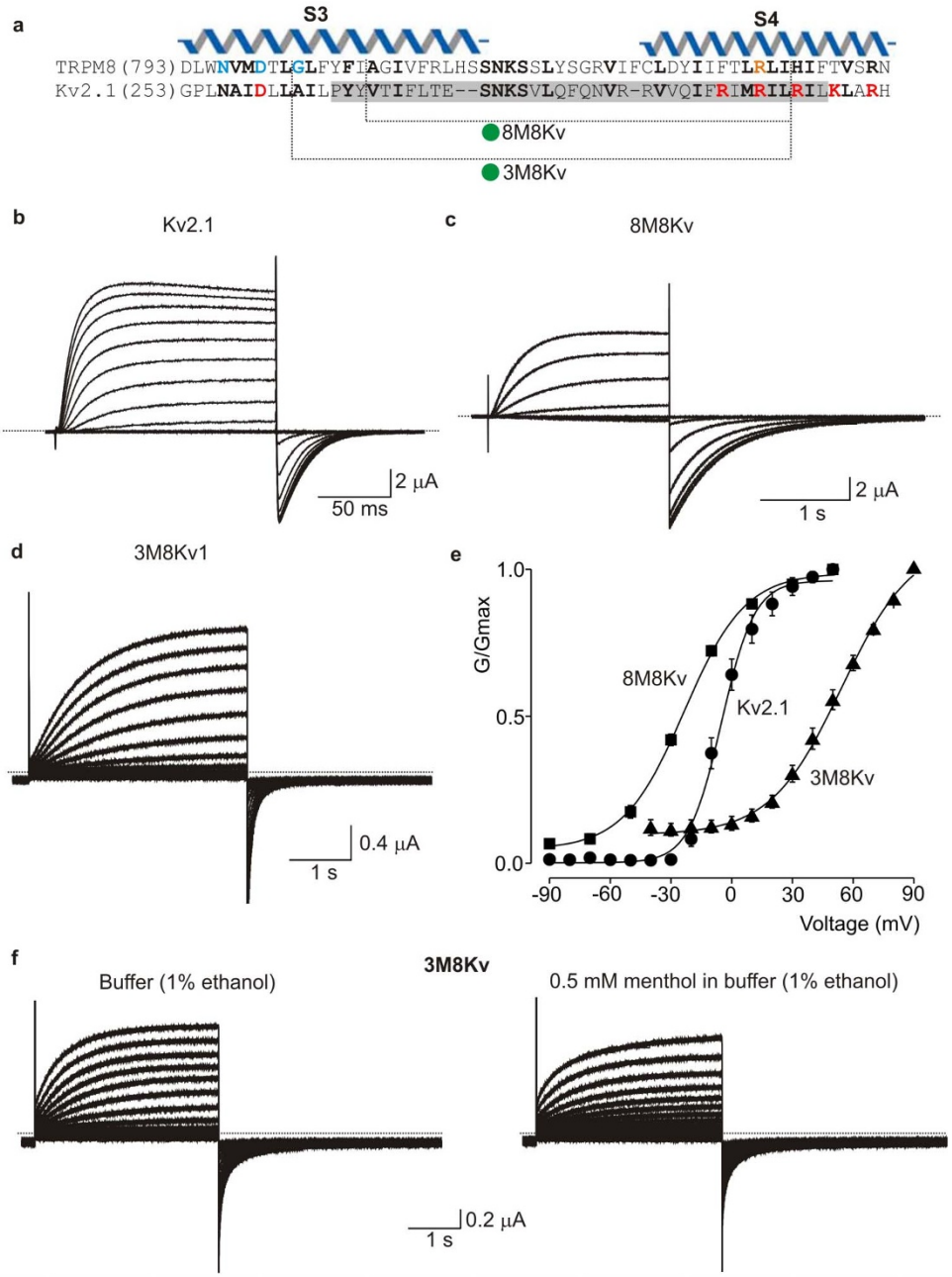

Figure 4 | Chimeras of S3–S4 region of TRPM8 transplanted into Kv2.1. (a) Alignment of TRPM8 and Kv2.1, and design of chimeras. (b) Families of current traces for Kv2.1 after subtraction of capacitive and leak currents using agitoxin2. Holding and tail voltages were −70 mV, and depolarizations were from −90 mV to +70 mV in 10 mV increments. (c) Families of current traces for 8M8Kv after subtraction of capacitive and leak currents using agitoxin2. Holding and tail voltages were −100 mV, and depolarizations were from −90 mV to +50 mV in 20 mV increments. (d) Families of unsubtracted current traces for 3M8Kv without subtraction of capacitive and leak currents. Holding and tail voltage was −70 mV, and depolarizations were from −40 mV to +90 mV in 10 mV increments. (e) G–V plots of Kv2.1 and the chimeras 3M8Kv and 8M8Kv. (f) Unsubtracted current traces for 3M8Kv before and after treatment with menthol. Voltage protocol was identical to the one used in d. Error bars indicate s.e.m. (n = 3). Dotted lines in current races represent zero current.

To explore this idea, we replaced portions of the S4 helix of TRPM8 (which has 2 Arg and 1 His) with those of the S4 helix of Kv2.1 (which has 6 positively charged residues). The chimera replacing the largest portion of the S4 helix in TRPM8 added one Arg residue, one Lys residue, and replaced a His with an Arg residue. However, all chimeras involving replacement of S3–S4 regions of TRPM8 with segments of the Kv2.1 paddle failed to give rise to either voltage- or menthol-activated currents (chimeras 1-4KvM8; Fig. 3).

S3–S4 chimeras between TRPV1 and Kv2.1. The sequence similarity between TRPV1 and Kv2.1 in the S3–S4 region is lower than that between TRPM8 and Kv2.1 (22% compared to 31%). Consequently, there are several alignments with similar homology that can be constructed between Kv2.1 and TRPV1. We therefore explored two alignments in the S3–S4 region to design chimeras between TRPV1 and Kv2.1 (Fig. 3a,b; 5a). In the first, the loop between the S3 and S4 helices of TRPV1 is longer than in the alternate alignment. Chimeras generated using both alignments gave rise to functional channels (2V1Kv, 5V1Kv, and 6V1Kv), with the exception of 1V1Kv. In contrast, when the same portion of the Kv2.1 paddle was replaced by the S3–S4 region of TRPV1 using the alternate alignment to generate chimera 5V1Kv, a functional Kv

Table 1 | Voltage-activation relationships for Kv2.1 and chimeras with TRPV1 and TRPM8

Channel	z	$V_{1/2}$ (mV)
Kv2.1	3.2 ± 0.3	−4.9 ± 0.9
3M8Kv	1.5 ± 0.1	54.2 ± 1.5
8M8Kv	1.7 ± 0.1	−23.4 ± 1.1
2V1Kv	0.9 ± 0.1	79.9 ± 0.7
5V1Kv	1.3 ± 0.1	70.3 ± 0.9

A single Boltzmann function was fit to G–V relations to obtain z and $V_{1/2}$ values. n = 3 in all cases.

channel was obtained (Fig. 5d and e), suggesting that the transferred region in this case was more compatible with the structure of Kv2.1 than for 1V1Kv. Similar to what was observed for the chimeras between Kv2.1 and TRPM8 discussed above, all functional chimeras were sensitive to agitoxin2, and had a reversal potential of ∼−20 mV.

Several of the functional paddle chimeras exhibited constitutive activity and could not be fully closed with membrane hyperpolarization even though they retained some voltage-sensitivity (for example, 2V1Kv and 6V1Kv; Fig. 5b, c, and e), resembling the 3M8Kv chimera discussed earlier. All these chimeras exhibit altered G–V relations, with slopes much lower than observed for Kv2.1 (Fig. 5e; Table 1). In the case of the 6V1Kv chimera, the G–V relation is so shallow and complex that it cannot be well-defined with a single Boltzmann function (Fig. 5e).

Residues in the S3–S4 region of TRPV1 shown in green in Fig. 5a have been demonstrated to be important for activation of the channel by capsaicin and RTX[9,10]. If these residues contribute to forming the receptor for these ligands, transferring the S3–S4 region of TRPV1 into Kv2.1 might render the chimeras sensitive to capsaicin. However, the largest of these chimeras (5V1Kv) was not sensitive to high concentrations of capsaicin even though it gave rise to robust voltage-activated currents (Fig. 5f). Similar to what we observed with TRPM8 chimeras, all reverse chimeras where portions of the S3–S4 region of TRPV1 were replaced by those of the Kv2.1 paddle failed to give rise to either voltage- or capsaicin-activated currents (1–4KvV1, Fig. 3).

Previous studies suggest that capsaicin binds to the internal regions between the S2 and S3 helices of TRPV1[8]. If this idea is correct, the lack of capsaicin sensitivity of the S3–S4 chimeras 2V1K, 5V1Kv, and 6V1Kv is not surprising as they do not contain any portion of the S2–S3 linker region of TRPV1. In an effort to render the Kv channel sensitive to capsaicin, we swapped the internal regions of the S2 and S3 helices in Kv2.1 with those of TRPV1 to generate the 8V1Kv chimera (Fig. 3). This chimera did not give rise to either voltage- or capsaicin-activated currents, suggesting that it is non-functional.

S1–S4 chimeras. The S1–S4 domain of Kv channels can be transferred to channels that are not voltage-activated, endowing them with voltage-sensitivity[41,42], demonstrating that the voltage sensor is an independent modular domain. Moreover, other voltage sensing proteins have been discovered that contain an S1–S4 domain without a separate pore domain, such as Ci-VSP[47], and Hv1[48,49]. Taken together, these observations suggest that nature utilizes the S1–S4 domain as a general scaffold to sense voltage. To test whether the S1–S4 regions of TRP channels have similar modular characteristics, we swapped the S1–S4 of TRPV1 and TRPM8 with that of Kv2.1, and also generated the reverse chimeras. All these chimeras (13M8Kv, 14M8Kv, 9V1Kv, 10V1Kv, 5KvM8, 6KvM8, 5KvV1 and 6KvV1 depicted in Fig. 3) did not give rise to voltage- or ligand-activated currents and were judged to be non-functional. We reasoned that these chimeras may have disrupted critical interactions between the S1 helix and pore helices of Kv2.1[50], resulting in a loss of channel function. To address this possibility, we created several S2–S4 chimeras, all of which were also non-functional (chimeras 15M8Kv, 11V1Kv, 7KvM8, and 7KvV1).

S5–S6 pore chimeras. In addition to serving as the ion permeation pathway, the pore region of TRP channels plays critical roles in channel gating and pharmacology. For example, the outer pore domains of TRPV1[13] and TRPV3[51] have been implicated in temperature sensing, and DkTx and the vanillotoxins are believed to activate TRPV1 by binding to its pore region[11,22,23]. Motivated by the putative functional importance of the pore domain in TRP channel function, we replaced the S5–S6 pore region of Kv2.1 with the pore regions of TRPV1 and TRPM8 (chimeras 16–18M8Kv and 12–14V1Kv; Fig. 3). We also generated the reverse chimeras (8–9KvM8 and 8–9KvV1; Fig. 3) where the pore regions of TRPV1 and TRPM8 were replaced by the Kv2.1 pore domain. However, none of these chimeras gave rise to voltage-activated currents, even for 17M8Kv, 18M8Kv, 13V1Kv and 14V1Kv, where the boundaries of the transferred region should not disrupt critical interactions between the S4–S5 linker and S6 helix defined for Kv channels[41,42]. We also investigated the DkTx-sensitivity of the three chimeras where the pore domain of Kv2.1 was replaced by that of TRPV1 (12–14V1Kv), but in each instance we could not observe measurable currents in response to application of 1 μM DkTx to the external recording solution, even when testing over a wide range of membrane voltages. Because heterologous expression of TRPV1 is more efficient in mammalian cells compared to oocytes, we transfected HEK-293 cells with a few of the chimeras (4KvV1, 5KvV1, 8KvV1, and 12V1Kv) and used whole-cell patch clamp recordings to look for evidence of functional channels. In these experiments, none of the chimeras gave rise to voltage-, capsaicin- or DkTx-activated currents that were distinguishable from non-transfected cells, confirming that they are non-functional.

Discussion

The primary objective of the present study was to establish structural relationships between TRP channels, for which little structural information is available, and Kv channels, for which a variety of X-ray structures have been solved[20,28,43]. One of the interesting findings in the present study is that transfer of S3–S4 regions of TRPV1 and TRPM8 into the paddle motif of Kv2.1 resulted in functional voltage-activated channels (Fig. 3, 4, and 5), even though this region of Kv2.1 and the two TRP channels has low sequence homology. When compared to the other "paddle chimeras" that have been generated and tested[32,34], our constructs possess the lowest sequence homology between the two proteins within the transferred region. Indeed, TRPM8 and Kv2.1 have a sequence similarity of 31% in the paddle region and TRPV1 and Kv2.1 have a sequence similarity of 22%, as compared to 40–45% between KvAP, Hv1, Nav2.1, Ci-VSP and Kv2.1. Our results strengthen the notion that Kv channel paddles lie in a remarkably unconstrained environment and probably make few critical contacts with the rest of the protein[19,20,28,30,32,34,52].

One interesting feature of several of the present paddle chimeras is that they displayed constitutive activity at negative membrane voltages (Fig. 4, 5). Constitutive activity has been observed in Kv channels with mutations in the S4–S5 linker or S6 helices, implicating those regions in coupling voltage-sensor movement and opening/closing of the internal S6 gate[41,42,53]. Constitutive activity has also been observed in the Shaker Kv channel, where multiple S4 arginine residues of the channel were neutralized and a voltage-independent conductance was observed[54]. In that case constitutive activity was only observed when three of the outer four arginine residues were neutralized at the R1, R2 and R4 positions, whereas our constitutively activated chimeras involved neutralization of R2 or R2 and R3. Kv2.1 already contains a glutamine at the R1 position, but has two additional arginine residues N-terminal to the canonical S4 arginine

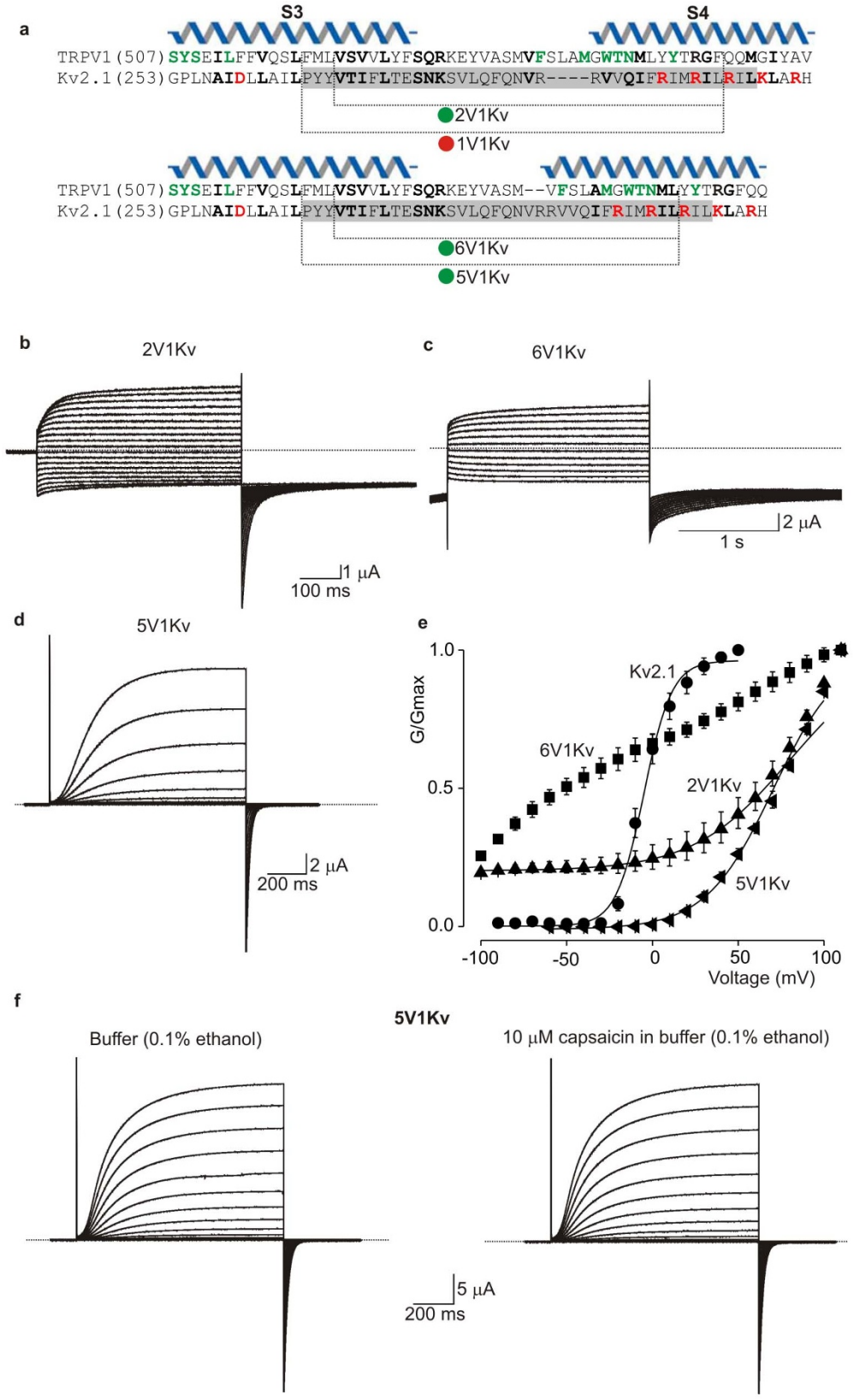

Figure 5 | Chimeras of S3–S4 region of TRPV1 transplanted into Kv2.1. (a) Alignments of TRPV1 and Kv2.1 and design of chimeras. (b) Families of current traces for 2V1Kv after subtraction of capacitive and leak currents using agitoxin2. Holding voltage was −20 mV, tail voltage was −100 mV and depolarizations were from −100 mV to +80 mV in 10 mV increments. (c) Families of current traces for 6V1Kv after subtraction of capacitive and leak currents using agitoxin2. Holding and tail voltage was −100 mV, and depolarizations were from −80 mV to +30 mV in 10 mV increments. (d) Unsubtracted families of current traces for 5V1Kv. Holding and tail voltage was −80 mV, and depolarizations were from −60 mV to +60 mV in 10 mV increments. (e) G–V plots of Kv2.1 and the chimeras. (f) Unsubtracted current traces for 5V1Kv before and after treatment with capsaicin. The voltage protocol was identical to the one used in d. Error bars indicate s.e.m. (n = 3). Dotted lines in current races represent zero current.

residues, both of which are neutralized in our constitutively active chimeras. Our chimeras also contain many other mutations in the transferred region, making it difficult to ascribe the constitutively activity to arginine neutralizations per se. Nevertheless, these collective results demonstrate that mutations in the voltage sensors, in addition to the S4–S5 linker and S6 gate can influence the coupling mechanism.

Although a strong indirect case can be made for structural similarities between TRP channels and Kv channels, as reviewed in the introduction, the vast majority of the chimeras we generated did not form functional channels. This outcome may help to explain why a majority of the functional chimeras involving TRP channels have been generated between orthologs of the same subtype. For example, chimeras between the rat and the avian orthologs of TRPV1 provided critical insights into the molecular determinants of vanilloid binding to the channel[8], and chimeras between rat and *Xenopus* TRPV1 provided evidence implicating the pore region of the channel as the binding site of DkTx[11]. Similarly, chimeras created between rat and chicken TRPM8 led to the identification of specific residues of TRPM8 that are involved in icilin sensitivity[17]. In contrast to these examples of functional chimeras between TRP channel orthologs, there are few reports on chimeras between TRP channels belonging to different subtypes. The prominent outliers include reports on TRPV1-TRPV2 chimeras[14,55] and those between TRPV1 and TRPM8[56]. Collectively, these results lead us to believe that the transmembrane regions of TRP channels have more constraining packing interactions than have been observed in X-ray structures of Kv channels[20,28,43], where S1–S4 domains are loosely associated with the central pore domain and the paddle motif is relatively unconstrained (Fig. 1b). We speculate the structures of transmembrane regions of TRP channels are more closely related to that observed in the X-ray structure of MlotiK[45], a prokaryotic tetrameric K channel containing a cytoplasmic cyclic nucleotide-binding domain, in which the helices within the S1–S4 domains exhibit extensive and tight packing interactions with each other and with the S5-S6 helices forming the central pore domain.

Methods

Channel constructs and chimera design. The Kv2.1Δ7 channel was used because this Kv2.1 construct is sensitive to agitoxin2[57], enabling the toxin to be used to identify currents associated with chimeras containing the pore region of this channel. The rat orthologs of TRPV1[58] and TRPM8[59] were utilized for all experiments, and were a generous gift from David Julius (UCSF). Chimeras were generated by utilizing an overlap PCR approach.

Chimeras between Kv2.1 and TRPV1/TRPM8 were designed based on the sequence alignments shown in Fig. 2 and 3. These alignments were generated by initially using the AlignX tool of the Vector NTI software (Invitrogen) to align the sequences of tetrameric six transmembrane cation channels and to S1–S4 containing proteins, including TRPV1, TRPM8, Kv2.1, Kv1.2, Shaker, KvAP, Ci-VSP, Hv1, rNav1.2, NavAb and MlotiK. The alignment thus generated was further adjusted manually to improve homology with transmembrane helices, in particular for residues known to be structurally and functionally critical in Kv channels. The start and end points of transmembrane regions for Kv1.2, KvAP, NavAb, and MlotiK were obtained by visualizing their respective high resolution crystal structures, and those for other channels shown in Fig. 2 were predicted based on their sequence alignments with these four proteins.

Electrophysiology. DkTx was produced recombinantly and agitoxin2 was synthesized by solid-phase methods as described previously[22]. Oocytes for chimera expression were obtained as previously described[53].

Two-electrode voltage-clamp recordings were performed using an OC-725C oocyte clamp amplifier (Warner Instruments). Data was filtered at 1 kHz (8 pole Bessel), and digitized at 10 kHz. Microelectrode resistances were between 0.1–1.2 MΩ when filled with 3 M KCl. Solutions for recording chimeras with the Kv channel pore contained (in mM) KCl (50), NaCl (50), $MgCl_2$ (1), $CaCl_2$ (0.3), and HEPES (20), at pH 7.4 (pH adjusted with NaOH). For recording currents from chimeras that contained TRP channel pores, $CaCl_2$ was replaced with $BaCl_2$. Unless otherwise stated, capacitive and background currents were identified by first blocking the Kv channel with agitoxin2, and then subtracting them to generate the currents shown in Fig. 4 and 5.

HEK-293 cells for whole-cell patch clamp recordings were split on glass coverslips in a six-well plate, transfected with 1 μg DNA per well and used 12–48 h after transfection. Whole-cell currents were recorded using an Axopatch 200 B patch clamp amplifier (Axon Instruments), filtered at 10 kHz (8 pole Bessel), and digitized at 50 kHz. Microelectrode resistances were between 1–4 MΩ when filled with pipette solutions. External solution for recording currents from the chimera with the Kv channel pore (8KvV1) contained (in mM) KCl (45), NaCl (100), $MgCl_2$ (0.5), $CaCl_2$ (2), and HEPES (10) at pH 7.2 (pH adjusted with NaOH), whereas the pipette solution contained (in mM) KCl (160), EGTA (1), $MgCl_2$ (0.5), and HEPES (10) at pH 7.4 (pH adjusted with NaOH). External solution for recording the chimeras with TRP channel pores (4KvV1, 5KvV1, and 12V1Kv) contained (in mM) KCl (2.8), NaCl (150), $MgSO_4$ (1), and HEPES (10) at pH 7.4 (pH adjusted with NaOH), whereas the pipette solution contained (in mM) $CsMeSO_3$ (130), CsCl (15), NaCl (4), EGTA (5), and HEPES (10), at pH 7.4 (pH adjusted with CsOH).

Conductance (G)–Voltage (V) relationships were obtained by measuring tail currents following depolarization to test voltages as indicated in Fig. 4 and 5. A single Boltzmann function was fitted to the data according to the equation, $G/G_{max} = [1 + \exp(-zF(V - V_{1/2})/RT)]^{-1}$.

1. Montell, C. & Rubin, G. M. Molecular characterization of the Drosophila trp locus: a putative integral membrane protein required for phototransduction. *Neuron* **2**, 1313–1323 (1989).
2. Gaudet, R. Divide and conquer: high resolution structural information on TRP channel fragments. *J Gen Physiol* **133**, 231–237 (2009).
3. Baez-Nieto, D., Castillo, J. P., Dragicevic, C., Alvarez, O. & Latorre, R. Thermo-TRP channels: biophysics of polymodal receptors. *Advances in experimental medicine and biology* **704**, 469–490 (2011).
4. Bohlen, C. J. & Julius, D. Receptor-targeting mechanisms of pain-causing toxins: How ow? *Toxicon* **60**, 254–264 (2012).
5. Ramsey, I. S., Delling, M. & Clapham, D. E. An introduction to TRP channels. *Annu Rev Physiol* **68**, 619–647 (2006).
6. Voets, T., Talavera, K., Owsianik, G. & Nilius, B. Sensing with TRP channels. *Nature chemical biology* **1**, 85–92 (2005).
7. DeFalco, J., Duncton, M. A. & Emerling, D. TRPM8 biology and medicinal chemistry. *Current topics in medicinal chemistry* **11**, 2237–2252 (2011).
8. Jordt, S. E. & Julius, D. Molecular basis for species-specific sensitivity to "hot" chili peppers. *Cell* **108**, 421–430 (2002).
9. Gavva, N. R. *et al.* Molecular determinants of vanilloid sensitivity in TRPV1. *J Biol Chem* **279**, 20283–20295 (2004).
10. Chou, M. Z., Mtui, T., Gao, Y. D., Kohler, M. & Middleton, R. E. Resiniferatoxin binds to the capsaicin receptor (TRPV1) near the extracellular side of the S4 transmembrane domain. *Biochemistry* **43**, 2501–2511 (2004).
11. Bohlen, C. J. *et al.* A bivalent tarantula toxin activates the capsaicin receptor, TRPV1, by targeting the outer pore domain. *Cell* **141**, 834–845 (2010).
12. Cui, Y. *et al.* Selective disruption of high sensitivity heat activation but not capsaicin activation of TRPV1 channels by pore turret mutations. *J Gen Physiol* **139**, 273–283 (2012).
13. Grandl, J. *et al.* Temperature-induced opening of TRPV1 ion channel is stabilized by the pore domain. *Nature neuroscience* **13**, 708–714 (2010).
14. Yao, J., Liu, B. & Qin, F. Modular thermal sensors in temperature-gated transient receptor potential (TRP) channels. *Proceedings of the National Academy of Sciences of the United States of America* **108**, 11109–11114 (2011).
15. Liu, B., Yao, J., Wang, Y., Li, H. & Qin, F. Proton inhibition of unitary currents of vanilloid receptors. *J Gen Physiol* **134**, 243–258 (2009).
16. Voets, T., Owsianik, G., Janssens, A., Talavera, K. & Nilius, B. TRPM8 voltage sensor mutants reveal a mechanism for integrating thermal and chemical stimuli. *Nature chemical biology* **3**, 174–182 (2007).
17. Chuang, H. H., Neuhausser, W. M. & Julius, D. The super-cooling agent icilin reveals a mechanism of coincidence detection by a temperature-sensitive TRP channel. *Neuron* **43**, 859–869 (2004).
18. Bandell, M. *et al.* High-throughput random mutagenesis screen reveals TRPM8 residues specifically required for activation by menthol. *Nature neuroscience* **9**, 493–500 (2006).
19. Swartz, K. J. Sensing voltage across lipid membranes. *Nature* **456**, 891–897 (2008).
20. Long, S. B., Tao, X., Campbell, E. B. & MacKinnon, R. Atomic structure of a voltage-dependent K+ channel in a lipid membrane-like environment. *Nature* **450**, 376–382 (2007).
21. Swartz, K. J. Tarantula toxins interacting with voltage sensors in potassium channels. *Toxicon* **49**, 213–230 (2007).
22. Bae, C. *et al.* High Yield Production and Refolding of the Double-Knot Toxin, an Activator of TRPV1 Channels. *PloS one* **7** (12): e51516. doi:10.1371/journal.pone.0051516 (2012).
23. Siemens, J. *et al.* Spider toxins activate the capsaicin receptor to produce inflammatory pain. *Nature* **444**, 208–212 (2006).
24. Hill, K. & Schaefer, M. TRPA1 is differentially modulated by the amphipathic molecules trinitrophenol and chlorpromazine. *J Biol Chem* **282**, 7145–7153 (2007).
25. Armstrong, C. M. Interaction of tetraethylammonium ion derivatives with the potassium channels of giant axons. *J Gen Physiol.* **58**, 413–437 (1971).
26. Jara-Oseguera, A., Llorente, I., Rosenbaum, T. & Islas, L. D. Properties of the inner pore region of TRPV1 channels revealed by block with quaternary ammoniums. *J Gen Physiol* **132**, 547–562 (2008).

27. Holmgren, M., Smith, P. L. & Yellen, G. Trapping of organic blockers by closing of voltage-dependent K+ channels: evidence for a trap door mechanism of activation gating. *J Gen Physiol* **109**, 527–535 (1997).
28. Jiang, Y. *et al.* X-ray structure of a voltage-dependent K+ channel. *Nature* **423**, 33–41 (2003).
29. Jiang, Y., Ruta, V., Chen, J., Lee, A. & MacKinnon, R. The principle of gating charge movement in a voltage-dependent K+ channel. *Nature* **423**, 42–48 (2003).
30. Ruta, V., Chen, J. & MacKinnon, R. Calibrated measurement of gating-charge arginine displacement in the KvAP voltage-dependent K+ channel. *Cell* **123**, 463–475 (2005).
31. Swartz, K. J. & MacKinnon, R. Mapping the receptor site for hanatoxin, a gating modifier of voltage- dependent K+ channels. *Neuron* **18**, 675–682 (1997b).
32. Alabi, A. A., Bahamonde, M. I., Jung, H. J., Kim, J. I. & Swartz, K. J. Portability of paddle motif function and pharmacology in voltage sensors. *Nature* **450**, 370–375 (2007).
33. Milescu, M. *et al.* Tarantula toxins interact with voltage sensors within lipid membranes. *J Gen Physiol* **130**, 497–511 (2007).
34. Bosmans, F., Martin-Eauclaire, M. F. & Swartz, K. J. Deconstructing voltage sensor function and pharmacology in sodium channels. *Nature* **456**, 202–208 (2008).
35. Milescu, M. *et al.* Interactions between lipids and voltage sensor paddles detected with tarantula toxins. *Nat Struct Mol Biol* **16**, 1080–1085 (2009).
36. Ahern, C. A. & Horn, R. Specificity of charge-carrying residues in the voltage sensor of potassium channels. *J Gen Physiol* **123**, 205–216 (2004).
37. Aggarwal, S. K. & MacKinnon, R. Contribution of the S4 segment to gating charge in the Shaker K+ channel. *Neuron* **16**, 1169–1177 (1996).
38. Seoh, S. A., Sigg, D., Papazian, D. M. & Bezanilla, F. Voltage-sensing residues in the S2 and S4 segments of the Shaker K+ channel. *Neuron* **16**, 1159–1167 (1996).
39. Salazar, H. *et al.* Structural determinants of gating in the TRPV1 channel. *Nat Struct Mol Biol* **16**, 704–710 (2009).
40. Liu, Y., Holmgren, M., Jurman, M. E. & Yellen, G. Gated access to the pore of a voltage-dependent K+ channel. *Neuron* **19**, 175–184 (1997).
41. Lu, Z., Klem, A. M. & Ramu, Y. Coupling between Voltage Sensors and Activation Gate in Voltage-gated K^+ Channels. *J Gen Physiol* **120**, 663–676 (2002).
42. Lu, Z., Klem, A. M. & Ramu, Y. Ion conduction pore is conserved among potassium channels. *Nature* **413**, 809–813 (2001).
43. Long, S. B., Campbell, E. B. & Mackinnon, R. Crystal structure of a mammalian voltage-dependent Shaker family K+ channel. *Science* **309**, 897–903 (2005).
44. Payandeh, J., Scheuer, T., Zheng, N. & Catterall, W. A. The crystal structure of a voltage-gated sodium channel. *Nature* **475**, 353–358 (2011).
45. Clayton, G. M., Altieri, S., Heginbotham, L., Unger, V. M. & Morais-Cabral, J. H. Structure of the transmembrane regions of a bacterial cyclic nucleotide-regulated channel. *Proceedings of the National Academy of Sciences of the United States of America* **105**, 1511–1515 (2008).
46. Garcia, M. L., Garcia-Calvo, M., Hidalgo, P., Lee, A. & MacKinnon, R. Purification and characterization of three inhibitors of voltage- dependent K+ channels from Leiurus quinquestriatus var. hebraeus venom. *Biochemistry* **33**, 6834–6839 (1994).
47. Murata, Y., Iwasaki, H., Sasaki, M., Inaba, K. & Okamura, Y. Phosphoinositide phosphatase activity coupled to an intrinsic voltage sensor. *Nature* **435**, 1239–1243 (2005).
48. Ramsey, I. S., Moran, M. M., Chong, J. A. & Clapham, D. E. A voltage-gated proton-selective channel lacking the pore domain. *Nature* **440**, 1213–1216 (2006).
49. Sasaki, M., Takagi, M. & Okamura, Y. A Voltage Sensor-Domain Protein is a Voltage-Gated Proton Channel. *Science* **312**, 589–592 (2006).
50. Lee, S. Y., Banerjee, A. & MacKinnon, R. Two separate interfaces between the voltage sensor and pore are required for the function of voltage-dependent K(+) channels. *PLoS biology* **7**, e47 (2009).
51. Grandl, J. *et al.* Pore region of TRPV3 ion channel is specifically required for heat activation. *Nature neuroscience* **11**, 1007–1013 (2008).
52. Xu, Y., Ramu, Y. & Lu, Z. A shaker K+ channel with a miniature engineered voltage sensor. *Cell* **142**, 580–589 (2010).
53. Sukhareva, M., Hackos, D. H. & Swartz, K. J. Constitutive activation of the shaker kv channel. *J Gen Physiol* **122**, 541–556 (2003).
54. Bao, H., Hakeem, A., Henteleff, M., Starkus, J. G. & Rayner, M. D. Voltage-insensitive gating after charge-neutralizing mutations in the S4 segment of Shaker channels. *J Gen Physiol* **113**, 139–151 (1999).
55. Jung, J. *et al.* Agonist recognition sites in the cytosolic tails of vanilloid receptor 1. *J Biol Chem* **277**, 44448–44454 (2002).
56. Brauchi, S., Orta, G., Salazar, M., Rosenmann, E. & Latorre, R. A hot-sensing cold receptor: C-terminal domain determines thermosensation in transient receptor potential channels. *The Journal of neuroscience* **26**, 4835–4840 (2006).
57. Li-Smerin, Y. & Swartz, K. J. Gating modifier toxins reveal a conserved structural motif in voltage- gated Ca2+ and K+ channels. *Proceedings of the National Academy of Sciences of the United States of America* **95**, 8585–8589 (1998).
58. Caterina, M. J. *et al.* The capsaicin receptor: a heat-activated ion channel in the pain pathway. *Nature* **389**, 816–824 (1997).
59. McKemy, D. D., Neuhausser, W. M. & Julius, D. Identification of a cold receptor reveals a general role for TRP channels in thermosensation. *Nature* **416**, 52–58 (2002).

Acknowledgments

We thank Miguel Holmgren, Andres Jara-Oseguera, Dmitriy Krepkiy, Mark Mayer, Joe Mindell and members of the Swartz lab for helpful discussions. This work was supported by the Intramural Research Program of the National Institutes of Health National Institute of Neurological Disorders and Stroke (to K.J.S.), and by a National Institutes of Health National Institute of Neurological Disorders and Stroke competitive fellowship (to J.K.).

Author contributions

J. K. and K. J. S. designed the experiments, J. K. performed the experiments, and J. K. and K. J. S. wrote the paper.

Additional information

Competing financial interests: The authors declare no competing financial interests.

How to cite this article: Kalia, J. & Swartz, K.J. Exploring structure-function relationships between TRP and Kv channels. *Sci. Rep.* **3**, 1523; DOI:10.1038/srep01523 (2013).